

# Scaling for vibrational modes of fractals tethered at the boundaries

Sonali Mukherjee\* and Hisao Nakanishi

*Department of Physics, Purdue University, W. Lafayette, IN 47907*

(October 22, 2018)

Using a recently introduced mapping between a scalar elastic network tethered at its boundaries and a diffusion problem with permanent traps, we study various vibrational properties of progressively tethered disordered fractals. Different scaling forms are proposed for different types of boundary tethering and numerical investigation of the scaling is performed by the approximate diagonalization of the corresponding large, sparse transition probability matrices. Rather different localization behaviors are found for the leading modes depending on the types of tethering.

## I. INTRODUCTION

In this work we consider the vibrational spectrum associated with the *scalar* elasticity of fractals when their boundaries are progressively tethered to immobile, external anchors. By scalar elasticity, we mean the vibrational problem where the local displacement variable  $u_i(t)$  at site  $i$  is a scalar. We study the various signatures of the vibrational density of states and the localization properties of the normal modes under these conditions.

The spatial scale invariance of fractals [1] and the absence of translational invariance due to the boundaries conspire to influence their vibrational spectra in fundamental ways. The now well-studied fracton [2] spectrum, with the characteristic, fractional power law for the low-energy density of states, arises for the bulk fractals with free boundaries, while so-called fractino [3] spectrum arises for objects which do not have fractal bulk but have fractal boundaries that are clamped. Here, we generalize these further to study bulk fractals whose fractal boundaries are progressively clamped or tethered to immobile anchors. The resulting vibrational spectrum is complex yet shows some simple scaling features common to many phenomena with long range order.

The problem of vibrations in a disordered system is in itself of physical interest. Granular systems [4], such as sand or snow piles or crops stored in silos, are among the systems of potential application. For example, sound propagation in a granular system had been modeled by Leibig [5] using a scalar elastic network with a random distribution of spring constants and analyzed in terms of the normal modes. Boundary conditions such as tethering add much complexity to the problem which may be relevant to some physical and engineering applications. For example, random mixtures of soft and hard materials such as solid granules embedded in a polymer gel or colloidal particles and aggregates filling the pores or cracks in rocks may constitute such an application. Another potential interest might be due to the recently discovered anomalous behavior [6] of the superfluid transition when aerogels [7] are embedded in liquid  $^4\text{He}$  or  $^3\text{He}$ , where the aerogels may impose a boundary condition over a fractal boundary of the liquid helium.

Most previous works on the effect of clamped boundaries on the vibrational density of states of inhomogeneous systems dealt with deterministic inhomogeneities (such as in *fractal drums* [3]). In this case the bulk is nonfractal (Euclidean) and the boundary is an ordered fractal, and the effect is a correction term to the leading behavior, the latter remaining the same as for a homogeneous system as one approaches the asymptotic limit of large system sizes. We have a substantially different system where both the bulk and the tethered boundaries are statistical fractals, sometimes of different fractal dimensionality, where even the leading behavior is expected to be special to inhomogeneous systems.

The prototype of such a system is a critical percolation cluster [8]. We have used site percolation clusters created near the critical percolation threshold on square and simple cubic lattices. We focus our attention on the low-energy regime where we expect the clamping effect of the fractal boundaries to be pronounced. Without tethering, these modes tend to have relatively large spatial extent, and thus are more sensitive to boundary tethering. In particular, we study the lowest energy mode ( $\epsilon_1$ ) and the peak ( $\epsilon_p$ ) that appears in the low-energy region of the vibrational density of states. The lowest energy mode is computationally much easier to obtain than the entire density of states and yet captures some of its essential features.

To study these systems, we exploit the mapping between scalar elasticity and diffusion as extended [9] to the case of mapping between the vibration of tethered objects and diffusion with permanent traps. In this approach, we define a transition probability matrix  $\mathbf{W}$  (an  $S \times S$  matrix for a cluster of  $S$  sites) where  $W_{ij}$  is the hopping probability per step  $p_{ij}$  from site  $j$  to site  $i$  in the corresponding diffusion problem. We set  $p_{ij} = 1/z$  for all pairs of nontethered sites  $i, j$  where  $z$  is the lattice coordination number. The diagonal elements  $W_{ii} = 0$  if site  $i$  is tethered (representing the complete leakage of diffusion field or *full* tethering) while, if  $i$  is not tethered,  $W_{ii} = 1 - n_i/z$  (representing conservation of diffusion field) where  $n_i$  is the number of available neighbors for site  $i$ . Then the time evolution of the diffusion field  $P_i(t)$  is given by

$$P_i(t+1) = \overline{\sum}_j [p_{ij}P_j(t) + (\delta_{ij} - p_{ji})P_i(t)] = \overline{\sum}_j W_{ij}P_j(t), \quad (1)$$

where  $\overline{\sum}$  includes the diagonal terms.

The eigenmodes of  $\mathbf{W}$  are the normal modes of the tethered vibration problem and the eigenvalues  $\lambda$  are related to the classical vibration frequency  $\omega$  and energy  $\epsilon \equiv \omega^2$  by

$$\lambda = 1 - \omega^2 \approx \exp(-\omega^2) \quad (2)$$

where the last approximation corresponds to the long time limit. We use this formulation in part to take advantage of the fact that the low-energy region of the spectrum corresponds to the region of the maximum eigenvalues of  $\mathbf{W}$  [10] which affords a much easier access numerically. The numerical technique used is based on the work of Saad [11] which implemented Arnoldi's method. Preliminary results of this work were reported earlier in [9] which introduced the

mapping as well as presented preliminary numerical results only for the *all boundary* tethered case in two dimensions. In the current work, we have improved data in both two and three dimensions as well as for *hull* tethering (see below).

## II. SCALING OF LOWEST ENERGY MODE FOR HULL VERSUS ALL BOUNDARY TETHERING

In a cluster with tethered boundaries the lowest energy mode  $\epsilon_1$  crucially depends on how many and which sites are tethered. Clearly, for an individual untethered mode, tethering of the sites where the mode has a large component greatly affects the mode. Statistically, an important classification of the boundary sites is between the internal and external boundaries (or *hull*) [12]. For a fractal like the critical percolation cluster, they are both fractal objects with similar (but not identical) fractal dimensions; in two dimensions, the hull has a fractal dimension  $d_f^h = 1.75$  while the internal boundaries have a fractal dimension  $d_f^i = 91/48$  (same as the bulk fractal itself and also as the fractal dimension of all boundary  $d_f^b$ ). However, the behavior of  $\epsilon_1$  (and the density of states) is unexpectedly different depending on if only (some of) the hull sites are tethered or (some of) both types of boundary sites (i.e., the hull and internal boundary) are tethered, as functions of the number  $N$  of the tethered sites and the size  $S$  of the cluster, the two main parameters in these situations.

In order to understand the interplay of the different length scales we write the scaling variable as the ratio of the relevant length scales for the two cases. The common length scale for both cases is the average distance  $l$  between the tethered sites where

$$l \sim (S/N)^{1/d_f}. \quad (3)$$

We also extend the meaning of  $N$  by  $N \equiv fN_T$  where  $f$  is the fraction of the  $N_T$  boundary sites which are tethered:  $N_T = N_h$  (number of hull sites) for hull tethering,  $N_T = N_a$  (number of all boundary sites) for all boundary tethering. In particular, this means  $N$  can be smaller than one if  $f$  is sufficiently small, which indicates many random samples in the ensemble will have no tethers.

The second relevant length scale  $L$  for hull tethering for the critical percolation cluster is the the average diameter of the cluster itself,

$$L_c \sim S^{1/d_f} \quad (4)$$

since the hull forms a connected set of external boundaries to whose interior the normal modes are confined. In particular, the spatial extent of the lowest energy mode is dictated by that of the interior sites at the scale of the cluster diameter  $L_c$ ). See the illustration of these lengths in Fig.1.

On the other hand, in the case of all boundary tethering, the second relevant length  $L_b$  is the average diameter of a *blob* in the cluster. As sites of both hull and internal boundary are tethered in *all* boundary tethering, a normal mode is confined to sites which are internal to both boundaries. i.e., in the blobs. The blobs in this context may be the areas of the cluster with essentially no internal holes (empty sites in the interior), which are connected together by links of less connectivity to form the overall cluster. See the illustration of these lengths in Fig.1. Though we do not have a precise characterization of a *blob*, it is clear that this sense of a blob is different from those discussed earlier, e.g., in the sense of a merely multiply connected component [13].

Since one would expect these new blobs to go critical at the ordinary critical percolation threshold  $p_c$ , its diameter  $L_b$  may be expected to follow a power law at  $p_c$ ,

$$L_b \sim S^y \quad (5)$$

for an appropriate universal exponent  $y$  in the scaling regime of large  $S$ . We note that both a precise identification of such blobs and the relation between  $L_b$  and  $S$  are still open questions [14].

Let us consider *scaling* for the hull tethering case first. In the limit of no tethering, the problem is reduced to that of so-called *ants* [10] where the lowest energy mode is the *stationary* mode with  $\epsilon = 0$  for any  $S$ . On the other hand, for asymptotically large  $S$  and fixed  $L_c/l > 0$  (i.e., fixed  $N > 0$  and  $S \rightarrow \infty$ ), the number of tethered sites  $N$  becomes negligible compared to cluster size  $S$ . Thus, the lowest energy mode is arbitrarily close to stationarity and should behave essentially in the same way as the second lowest energy mode (lowest energy, nontrivial mode) of the nontethered case, i.e., as  $\epsilon_1 \sim S^{-d_w/d_f}$  ( $d_w$  is the *walk dimension* and  $d_f$  is the fractal dimension of the cluster). Thus, the scaling form of  $\epsilon_1$  is expected to be

$$\epsilon_1 \sim S^{-d_w/d_f} F(L_c/l) = S^{-d_w/d_f} G(N). \quad (6)$$

Since  $\epsilon_1 \rightarrow 0$  as  $N \rightarrow 0$  with fixed  $S$ , we must have  $G(z) \rightarrow 0$  as  $z \rightarrow 0$ . If we assume analyticity of  $G(z)$  for small  $z$ , in the absence of obvious symmetry requirements which might remove the linear term, it seems reasonable to conclude  $G(z) \sim z$  for small  $z$ .

It is possible to obtain the limit of  $z \rightarrow \infty$  in such a way as to essentially remove the effect of tethering simultaneously. To this end, consider joining many mini-clusters with a given individual  $l_1$  in such a way so as to make the overall cluster a fractal with fractal dimension  $d_f$ . In this process the overall cluster length scale  $L_c$  increases at a greater rate ( $L_c \sim S^{1/d_f}$ ) than the overall  $l$  ( $l \sim (S/N)^{1/d_f}$ ) (since  $N$  is also growing). Thus, as more mini-clusters are joined, the variable  $L_c/l$  tends to  $\infty$  while the tethered hull ( $S^{d_f^h/d_f}$ ) becomes a negligible part of the entire boundary which goes as  $S$  (since  $d_f^h < d_f$ ). In this case with the diminished importance of tethered hull, the behavior of  $\epsilon_1$  should converge toward the lowest nontrivial mode of the nontethered limit once again ( $\epsilon_1 \sim S^{-d_w/d_f}$ ). Thus, in this limit of  $z = N \rightarrow \infty$ , the lowest eigenmode is confined *entirely* to the interior of the cluster, and the spatial extent and the energy of the mode is unaffected by further tethering of hull sites. This is equivalent to *herding* [9] which is a term we had used to describe the saturation effect of the confinement of an eigenmode. Thus, we must have  $G(z) \rightarrow \text{const.}$  as  $N \rightarrow \infty$ .

Next we consider all boundary tethering. The no-tethering limit is of course the same as for the hull tethering case. As one tethers sites of all boundaries, the lowest-energy mode gets localized in blobs which are unaffected by tethering. Moreover, if the ratio  $L_b/l$  is fixed at a nonzero value and  $S \rightarrow \infty$ , then each *blob* behaves like a cluster of its own with hull tethering. The expected scaling variable is then the number of tethered sites per blob  $NL_b^{d_f}/S$  (which is equal to  $(L_b/l)^{d_f}$  as expected). We thus propose a scaling form

$$\epsilon_1 \sim S^{-d_w/d_f} \overline{F}(L_b/l) = S^{-d_w/d_f} \overline{G}(N/S^x), \quad (7)$$

where  $x = 1 - yd_f$ .

For  $z \rightarrow 0$ , as for the hull tethering, we have  $\overline{G}(z) \rightarrow 0$ . However, the limit of  $z \rightarrow \infty$  can be achieved by increasing the fraction of tethered boundary sites as the cluster size increases. The limit should then correspond to the so-called *ideal chain* [10] with all the boundary sites tethered. Thus, in this limit,  $N \sim S$  and  $\epsilon_1 \sim (\ln S)^{-2/d_0}$  [15] (where  $d_0$  is the exponent describing the stretched exponential behavior of the density of states for ideal chains introduced in [16]). Numerically,  $d_0$  is about 4 in two dimensions and about 6 in three dimensions for the critical percolation cluster. Thus, the scaling function  $\overline{G}(z) \sim z^{d_w/[d_f(1-x)]} (\ln z)^{-2/d_0}$  as  $z \rightarrow \infty$ .

It is interesting to consider the connection of this behavior to the confinement of the lowest energy mode to the small, compact regions of the cluster in this case. These regions are not affected by tethering because of the absence of internal boundaries (holes). Their fractal dimension must be essentially equal to the Euclidean lattice dimension  $d$ . Thus, we denote their average size by  $S_c$ , we may expect  $\epsilon_1 \sim S_c^{-2/d}$  where 2 is the walk dimension on a compact cluster. In view of the relation  $\epsilon_1 \sim (\ln S)^{-2/d_0}$  above, this would lead to  $S_c \sim (\ln S)^{d/d_0} \approx (\ln S)^{1/2}$  in both two and three dimensions. This type of slow growth of  $S_c$  is consistent with our direct observations.

Fig.2 and Fig.3 show the numerical results for the above discussed scaling behavior for the square lattice in two dimensions. Fig.2 is for the hull tethering case while Fig.3 is for all boundary tethering. Besides the scaling variables on the  $x$  axis being different, the scaling functions exhibit dramatically different behavior. Though, in both cases,  $\epsilon_1$  (and thus the scaling functions) approach zero as  $z \rightarrow 0$ , the low  $z$  behavior is linear for hull tethering while it seems to be faster than linear for all boundary tethering. Also while the hull tethering scaling function tends to a finite limit as  $z \rightarrow \infty$  (see above discussion), that for all boundary tethering appears to grow unbounded as it should if  $x < 1$ . Corresponding results for all boundary tethering for the simple cubic lattice are shown in Fig.4. Here the reasonable data collapsing is achieved for  $x = 0.4$ .

We find, in particular, that hull tethering cannot change the behavior of the lowest energy mode, which remains the same as that of the untethered case ( $\epsilon_1 \sim S^{-d_w/d_f}$ ). This is because a fully tethered hull confines the mode in the interior of the critical percolation cluster which, asymptotically for large clusters, scales with the same fractal dimension as the entire cluster itself. Thus, the lowest energy mode results in the vibration of the interior of the cluster independent of the external boundary. This inability to change the behavior of the lowest energy mode is analogous to the case of an Euclidean cluster as well as to the fractal drums (fractal external boundary and Euclidean interior) [3].

In contrast, the tethering of all boundaries leads to confinement of the lowest energy vibrational mode in regions of the cluster which are essentially compact, altering its behavior from a power-law dependence on cluster size  $\epsilon_1 \sim S^{-d_w/d_f}$  to a slow logarithmic dependence on  $\epsilon_1 \sim (\ln S)^{-2/d_0}$ . Thus all boundary tethering conspires with the complex geometry of the critical percolation cluster (with pockets of compact regions, etc.) to dramatically alter the behavior of lowest energy vibrational mode.

### III. SCALING OF THE MAXIMUM IN DENSITY OF STATES

Let us now consider the vibrational density of states  $\rho(\epsilon)$  of the matrix  $\mathbf{W}$ . For nontethered limit,  $\rho(\epsilon)$  generally has a power law increase toward the lowest energy (stationary) mode [17]. On the other hand, if all boundary sites are tethered, we recover the *ideal chain* result of a stretched exponential *decrease* toward the lowest energy mode  $\epsilon_1$  [16]. Thus, when progressively more of all boundary sites are tethered, a crossover between the two limits occurs. For an intermediate fraction  $f$  of tethered sites, we generally observe a maximum in the density of states as shown in Fig.5(a) for the square lattice. Starting from larger  $\epsilon$  and moving toward  $\epsilon = 0$ ,  $\rho$  increases initially because the nontethered modes for the range of  $\epsilon$  are too localized to be affected when tethers are added, while for much smaller  $\epsilon$  the tethers begin to drag down the density of states. (Remember that tethers correspond to traps and low  $\epsilon$  corresponds to the long time survival of a diffusing particle.) Thus a peak in  $\rho(\epsilon)$  occurs, say, at  $\epsilon_p$ , which gradually increases from 0 for  $f = 0$  (*ant* limit) toward  $f = 1$  (ideal chain limit) as the tethering fraction  $f$  increases.

The existence of the maximum in the density of states has implications on the possible resonant behavior in response to the external source of vibrational energy. See Leibig [5] for a discussion of this point for the case of weakly disordered network of Hookian springs.

For the hull tethering case, the situation is similar for finite  $S$ . In the asymptotic large  $S$  limit, however, hull tethering cannot affect the density of states in qualitative manner no matter how large the tethering fraction  $f$  may be because the hull becomes increasingly a negligible fraction of all boundaries. This implies that, for large  $S$ , the region near  $\epsilon = 0$  must always witness power-law increasing  $\rho(\epsilon)$ . However, the finite  $S$  effect often masks this asymptotic behavior so that for most sizes of clusters numerically generated and for most tether fraction  $f$ , we do observe a maximum in the density of states similar to the all boundary tethering case (see Fig.5(b)).

The crossover of  $\epsilon_p$  as the tether fraction  $f$  is varied is then expected to obey the same type of scaling as for the lowest energy mode  $\epsilon_1$ . For hull tethering,

$$\epsilon_p \sim S^{-d_w/d_f} G_p(N), \quad (8)$$

while, for all boundary tethering,

$$\epsilon_p \sim S^{-d_w/d_f} \bar{G}_p(N/S^x), \quad (9)$$

with the same value of  $x$  as in Eq.(7).

These scaling laws have been tested on the same critical percolation clusters as for the lowest energy mode scaling. The numerical results, shown in Fig.6 for the hull case and Fig.7 for all boundary tethering, are in good agreement with the scaling laws above. The corresponding results for the simple cubic lattice in three dimensions are shown in Fig.8, again with reasonably good agreement when a choice of  $x = 0.4$  is used.

### IV. SPATIAL EXTENT OF THE LOWEST ENERGY MODE

The difference between hull and all boundary tethering is dramatic also in the spatial characters of the normal modes. We show in Fig.9 and Fig.10 the amplitude maps of typical lowest energy modes (corresponding to  $\epsilon_1$ ) for hull tethering and all boundary tethering, respectively. For hull tethering, starting from low tethering fraction  $f$  (or small  $N$ ) and increasing  $f$  initially reduces the amplitude of vibration of the sites in the vicinity of the tethered hull sites. This causes a decrease in the wavelength and consequently an increase in  $\epsilon_1$  (also of the scaling function  $F(z)$ ). However after a certain number of hull sites are tethered, the amplitudes of the mode at all sites near the hull become attenuated and the region of large amplitudes becomes well confined to the interior of the cluster. Beyond this point, increasing  $N$  does not further affect the spatial structure of the normal mode as the sites with appreciable amplitudes are already deeply in the interior of the cluster. This saturation behavior may be likened to herding of livestock into a safe, fenced haven, and thus we may call it *herding* of normal modes. Herding is reflected in the saturation behavior of  $F(z)$  for  $z$  tending to *infinity*. In the examples shown in Fig. 9, the participation ratios indicate that only about 1% of the sites contribute substantially to the mode for all shown values of the tethering fractions.

For all boundary tethering, increasing  $f$  serves to progressively confine the (originally most extended, untethered) normal mode to sites which are interior to both the external and internal boundaries, i.e., in the *blobs* of the percolation cluster. Since typically most blobs are very small, this results in a much sharper decrease in the spatial extent of the normal mode, as seen in Fig.10. Even for relatively small  $f$ , the effect of confinement can be nearly complete in this case, and further tethering may force the mode to jump around to distant locations which may allow the largest spatial extent. This behavior may be likened to chasing wild animals in a hunting expedition, and thus we may call it *hunting* of normal modes. It is interesting to note that, while the largest modes without tethering are those of

small  $\epsilon$ , they are also the ones most affected by tethering (particularly all boundary tethering), and thus after some tethers have been put in place, these modes are not necessarily the spatially largest ones any longer. Indeed those modes shown in Fig.10 have main contributions only from less than 0.1% of the sites according to the values of the participation ratios.

The above observations on the spatial structure of normal modes under boundary tethering may have technological implications. For example, a soft glassy material may need to be clamped only at relatively few locations on its external boundary to fully confine its lowest energy normal mode to its interior via *herding*.

## V. CONCLUSION

The present work reveals a number of interesting features of the elastic properties of a fractal with tethered boundaries. The vibrational modes and consequently the vibrational density of states for both hull and all boundary tethering are dictated by regions of clusters which are *tether free*. Despite the structural similarity between the hull and internal boundaries, the effect of tethering depends greatly on whether only the hull is tethered or all boundaries are tethered. Tethering of hull sites confines the low-energy vibrational modes in the interior of the cluster and since the interior of the cluster is itself a fractal with the fractal dimension same as that of the entire cluster, the leading behavior of the vibrational density of states for fully tethered hull must asymptotically be the same as that of the untethered cluster. On the other hand, for full tethering of all boundaries, the low-energy modes are confined in the compact regions of the cluster which, because of their small spatial extent, give rise to faster than exponential decrease in the density of states in the same limit.

Keeping in mind the fact that Euclidean clamped boundaries do not have an appreciable effect on the density of states, our results demonstrate the potential of tethering fractal boundaries to attenuate harmonic excitations. Also, the present problem is equivalent to that of diffusion in the presence of permanent traps, a fact that was taken advantage of for the numerical part of this work. Since the latter serves as a model for diffusion controlled reaction/absorption in the presence of immobile reactants/absorbents, there may also be applications in the areas of drug reaction/absorption, etc. Finally, because of the similar mathematical formulation of quantum mechanical localization and hopping transport problems [18], we expect that the same techniques will be useful in studying those problems and that some of the current results may have direct analogs in them.

---

\* Present Address: Department of Physics, University of West Virginia, Morgantown, WV 26506.

- [1] See, e.g., *Fractals*, J. Feder (Plenum, New York, 1988).
- [2] S. Alexander and R. Orbach, *J. Phys. Lett. (Paris)* **43**, 625 (1982).
- [3] B. Sapoval, Th. Gobron, and A. Margolina, *Phys. Rev. Lett.* **67**, 2974 (1991).
- [4] See, e.g., H. J. Herrmann, *Physica A* **191**, 263 (1992).
- [5] M. Leibig, *Phys. Rev. E* **49**, 1647 (1994).
- [6] G. K.-S. Wong, P. A. Crowell, H. A. Cho, and J. D. Reppy, *Phys. Rev. B* **48**, 3858 (1993).
- [7] E. Courtens, R. Vacher and E. Stoll, in *Fractals in Physics*, A. Aharony and J. Feder, eds. (North-Holland, Amsterdam, 1989).
- [8] D. Stauffer and A. Aharony, *Introduction to Percolation Theory* (Taylor and Francis, London, 1992).
- [9] S. Mukherjee and H. Nakanishi, *Fractals* **4**, 273 (1996).
- [10] See, e.g., H. Nakanishi in *Annual Reviews of Computational Physics Vol.I*, ed. D. Stauffer (World Scientific, Singapore, 1994).
- [11] Y. Saad, *Linear Algebra Appl.* **34**, 269 (1980) and W. E. Arnoldi, *Quart. Appl. Math.* **9**, 17 (1951).
- [12] B. Sapoval, M. Rosso, and J. F. Gouyet, *J. Phys. Lett. (Paris)* **46**, 149 (1985).
- [13] A. Coniglio, *J. Phys. A* **15**, 3829 (1982).
- [14] See, e.g., E. Cuansing, J. H. Kim and Hisao Nakanishi, to be published in *Phys. Rev. E* (1999) for the dynamic exponents of the percolation of high connectivity sites.
- [15] S. Mukherjee and H. Nakanishi, *Phys. Rev. E* **53**, 1470 (1996).
- [16] A. Giacometti and H. Nakanishi, *Phys. Rev. E* **50**, 1093 (1994), see also A. Giacometti, H. Nakanishi, A. Maritan and N. H. Fuchs, *J. Phys. A* **25**, L461 (1992).
- [17] S. Mukherjee, H. Nakanishi, and N. Fuchs, *Phys. Rev. E* **49**, 5032 (1994), and references therein.
- [18] T. Odagaki, N. Ogita, and H. Matsuda, *J. Phys. C*, **13**, 189 (1980).

FIG. 1. The average distance  $l$  between tethered sites, average diameter of the cluster  $L_c$ , and the average *blob* diameter  $L_b$ , for (a) all boundary tethering and (b) hull tethering.

FIG. 2. Scaling of the lowest energy mode for hull tethering on square lattice. Scaling variable reduces to  $N$ , which is the total number of tethered hull sites.

FIG. 3. Scaling of the lowest energy mode for all boundary tethering on square lattice. The scaling variable is  $N/S^x$  where  $x$  is numerically about 0.54.

FIG. 4. Scaling of the lowest energy mode for all boundary tethering on simple cubic lattice. The scaling variable is  $N/S^x$  where  $x$  is numerically about 0.4.

FIG. 5. (a) Density of energy eigenvalues are shown for all boundary tethering of 5000-site clusters at the tethering fraction of 0.1, 0.4, and 0.6. (b) shows the same for hull only tethering at fraction 0.3, 0.5, and 0.9.

FIG. 6. Scaling of the peak in the density of states for hull tethering on square lattice.

FIG. 7. Scaling of the peak in the density of states for all boundary tethering on square lattice.

FIG. 8. Scaling of the peak in the density of states for all boundary tethering on simple cubic lattice.

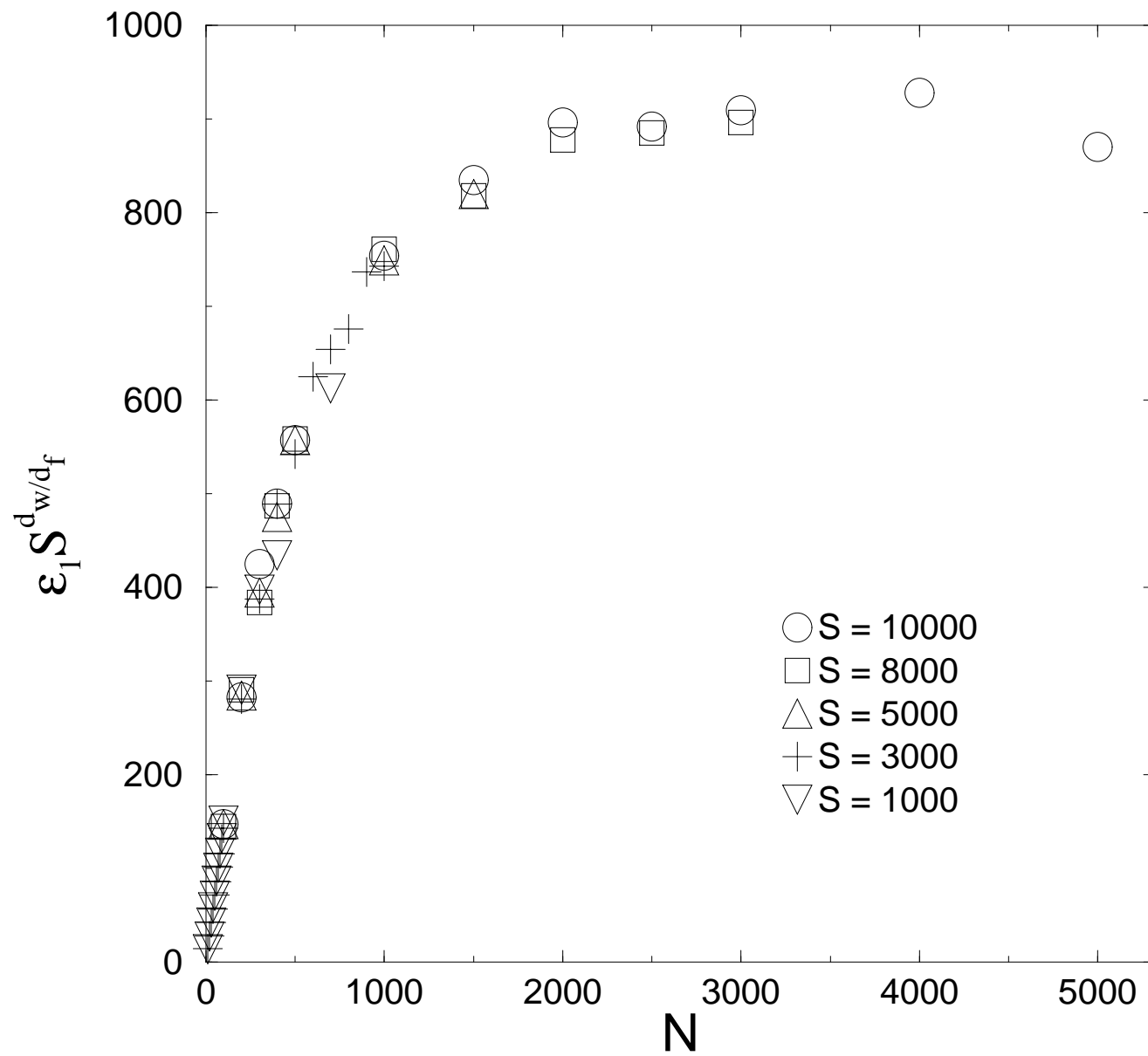
FIG. 9. Spatial extent of the lowest energy mode is illustrated by plotting the amplitudes of the mode for a 50000 site cluster on the square lattice for progressively increasing hull tethering fraction. Grey scale is used where lightest grey is used for the lowest (absolute value of) amplitude and black for the highest, in logarithmic scale. (a) corresponds to random tethering of 20% (upper left), (b) to 40% (upper right), (c) to 70% (lower left), and to 100% (lower right). Note that with zero tethering, the amplitude will be completely uniform.

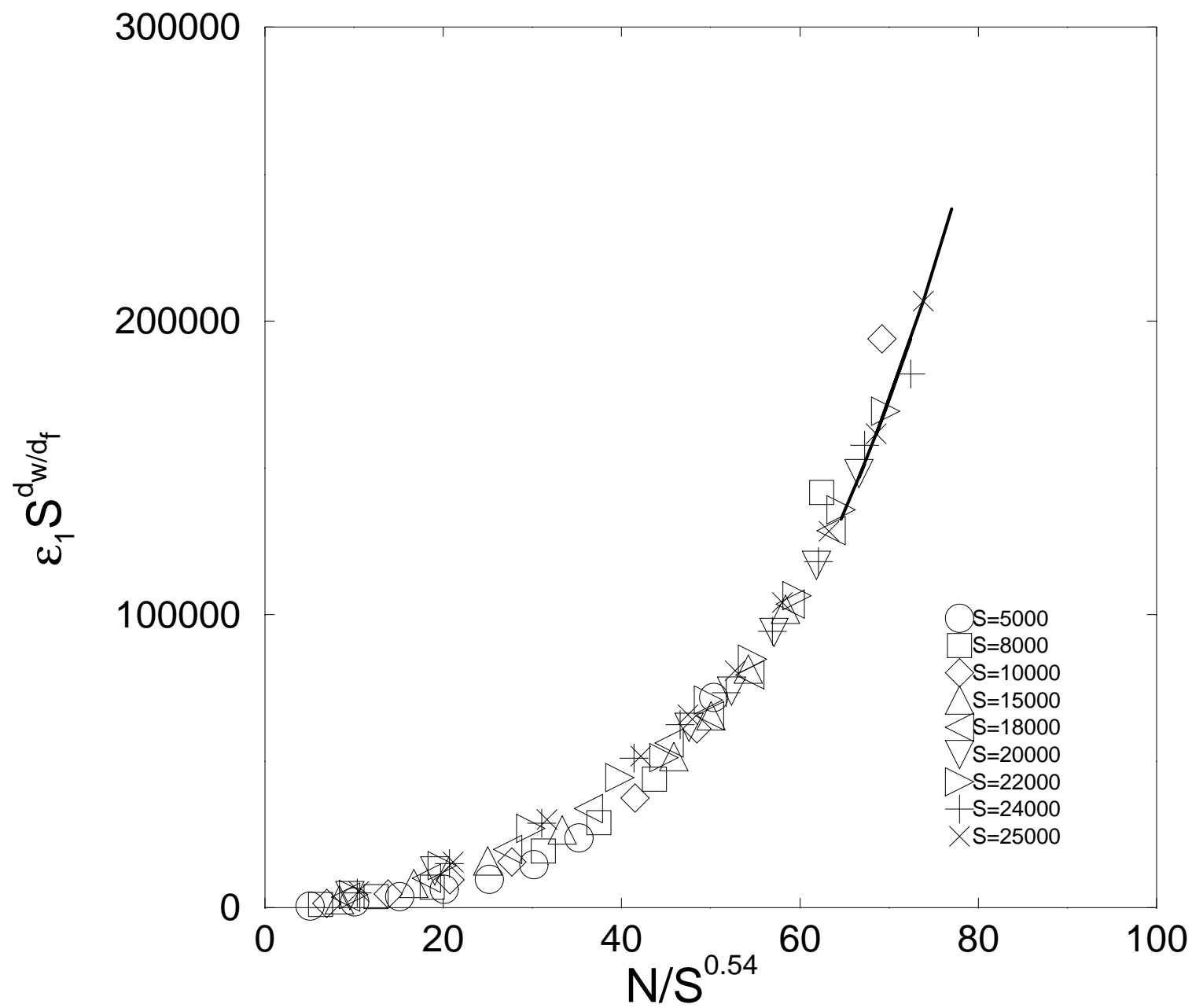
FIG. 10. Same as Fig.9 but for the all boundary tethering case.

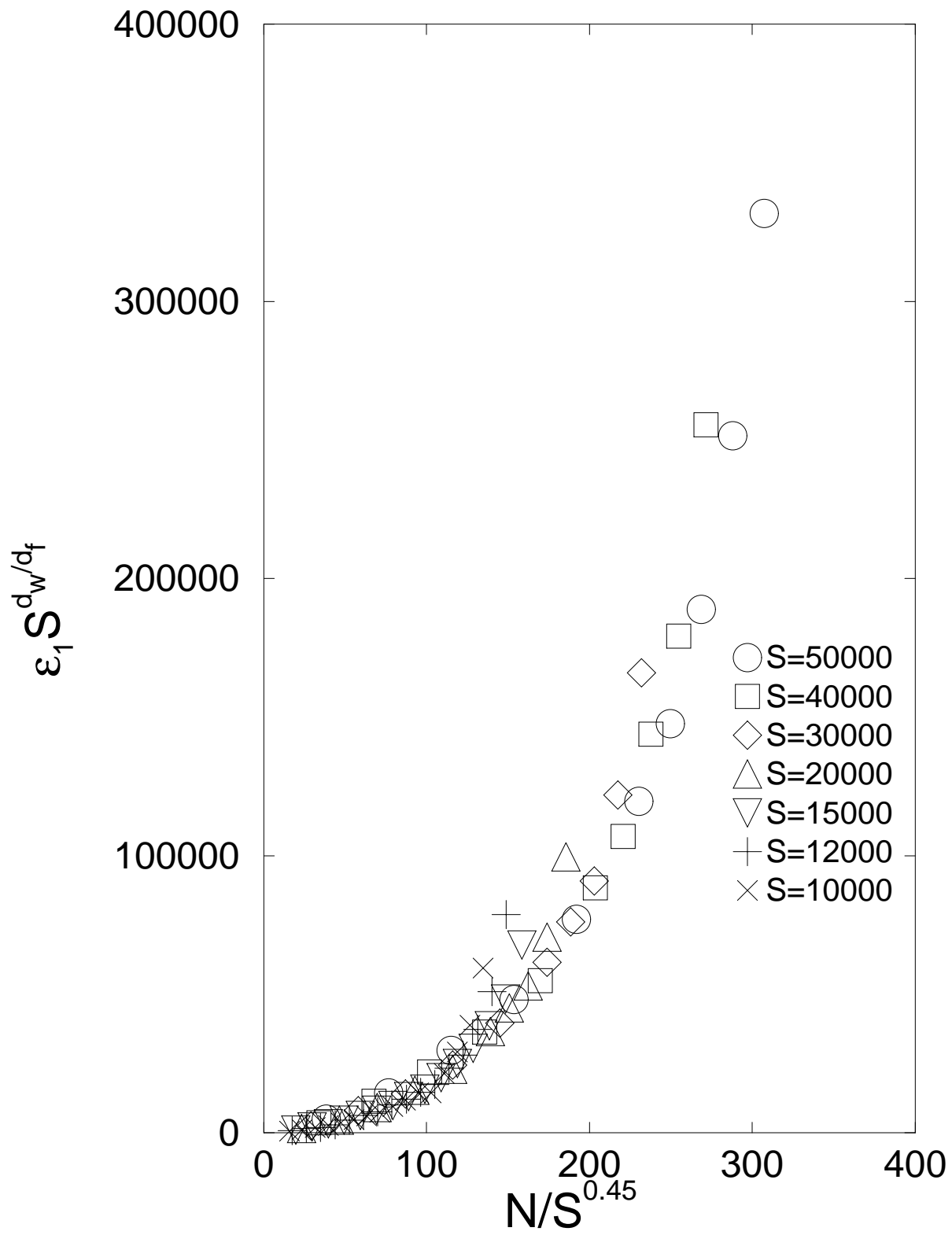
This figure "fig1.gif" is available in "gif" format from:

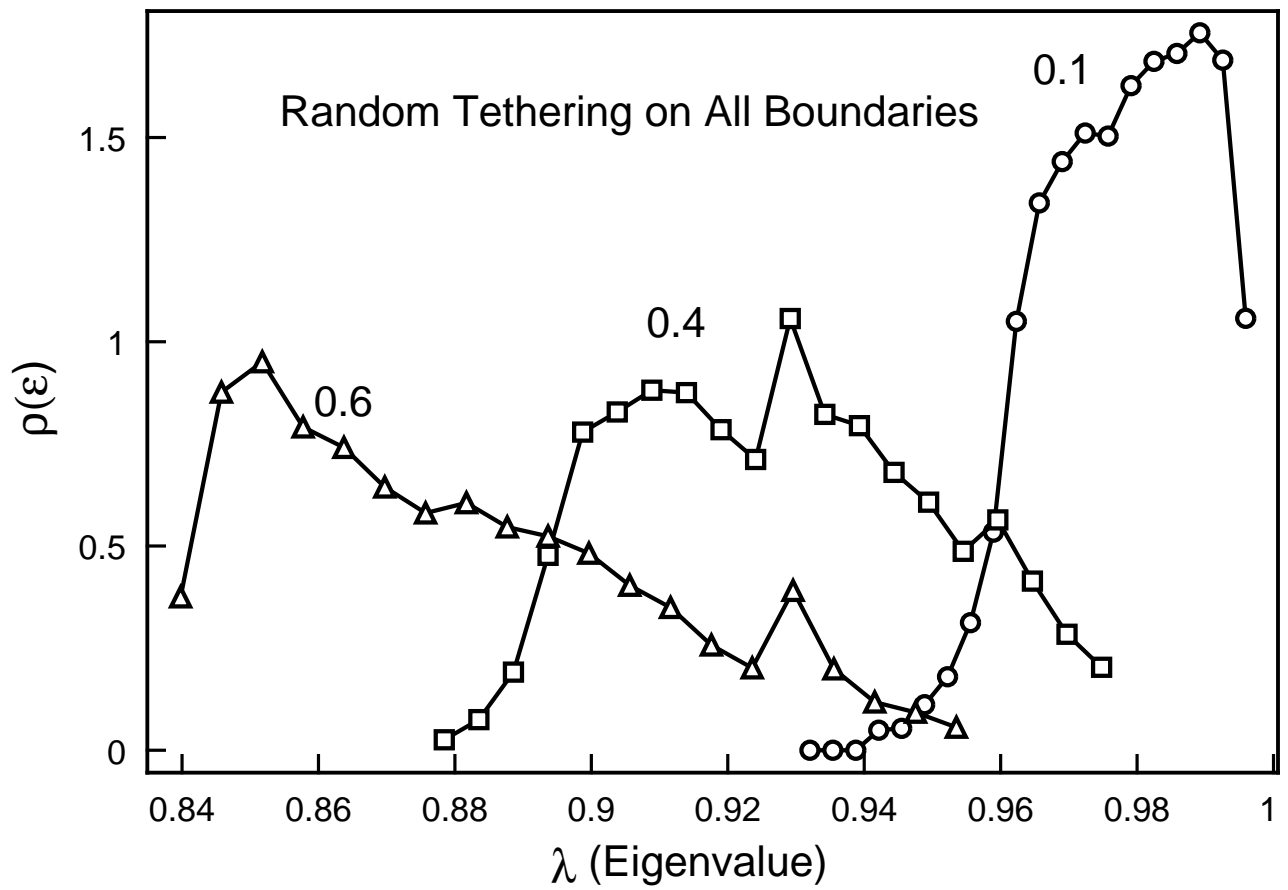
<http://arxiv.org/ps/cond-mat/9910138v1>

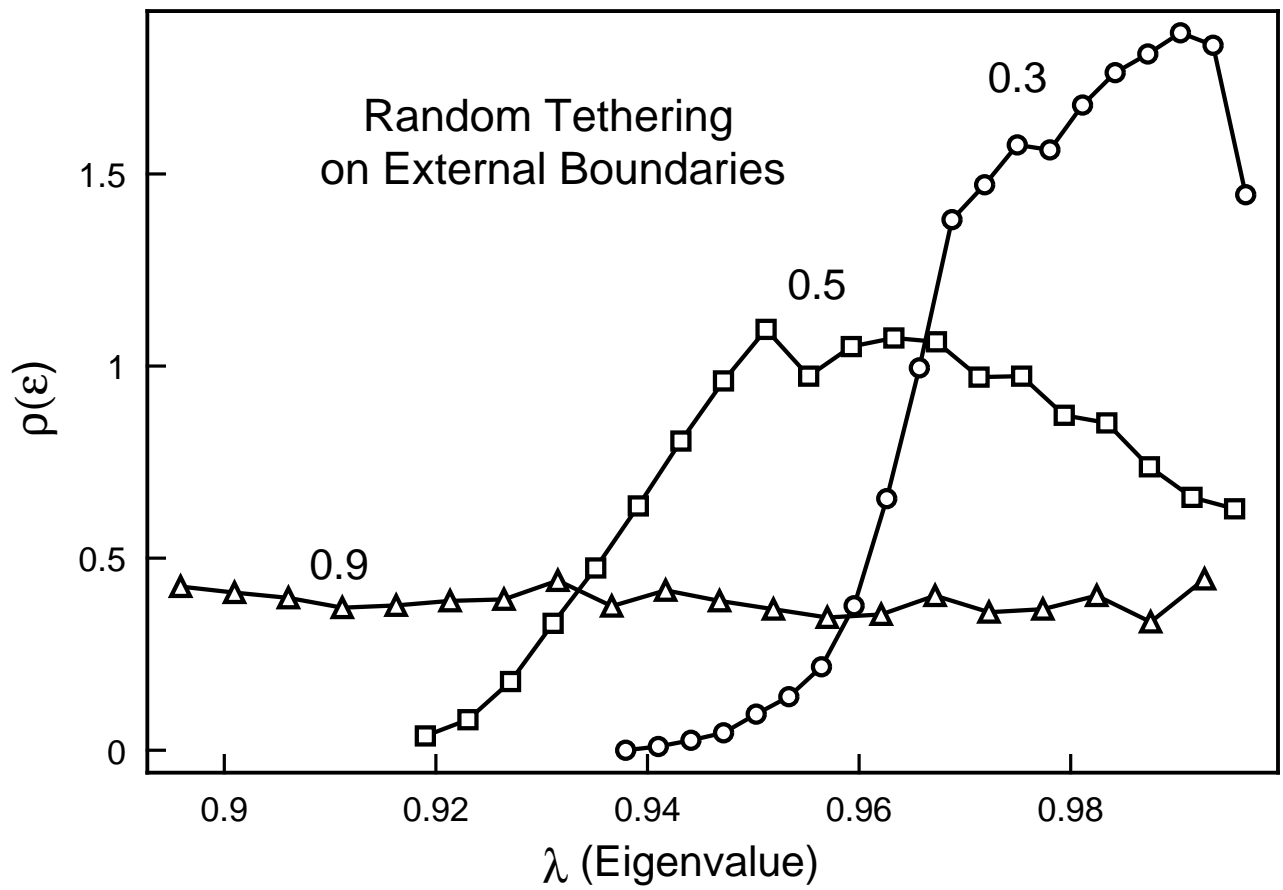


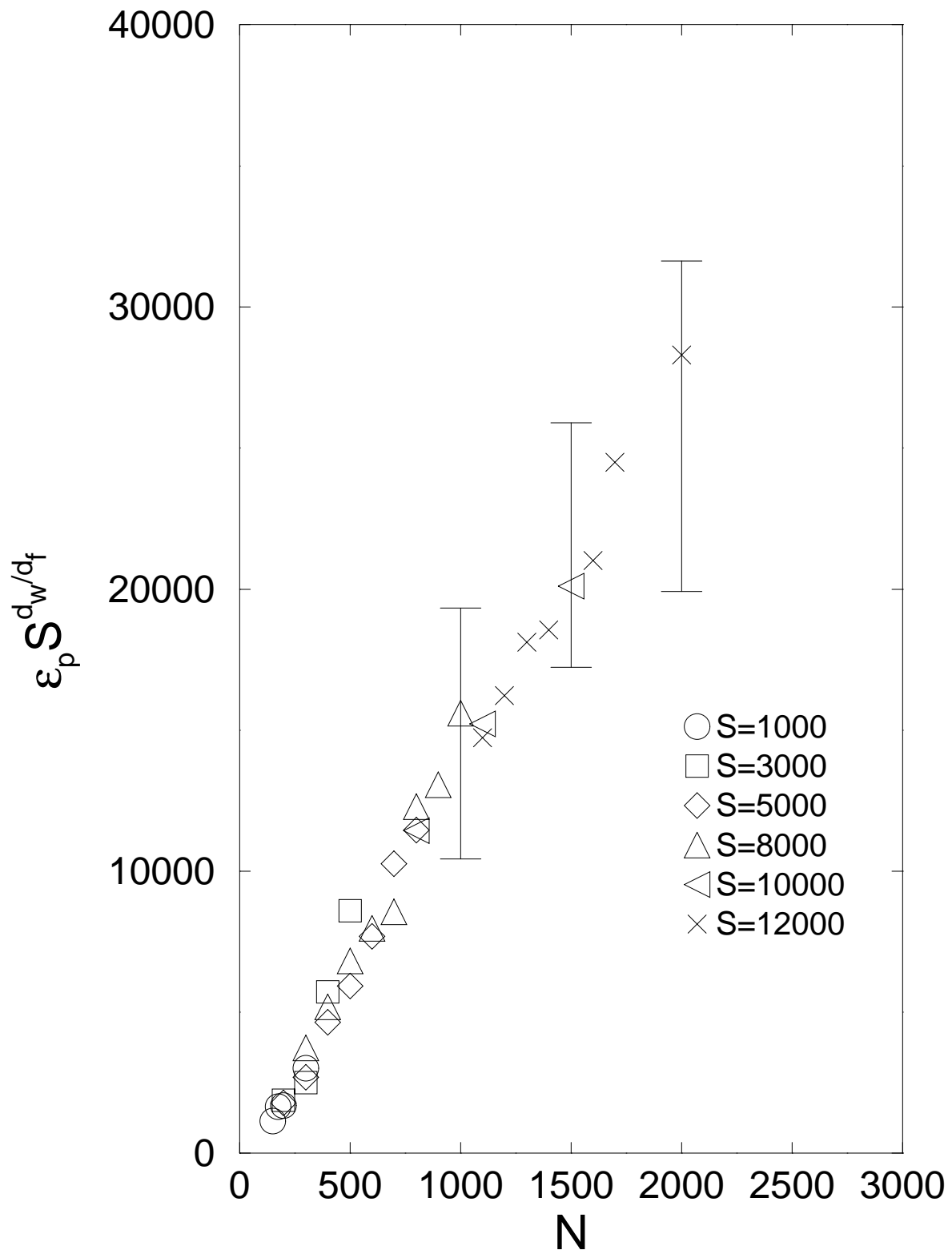


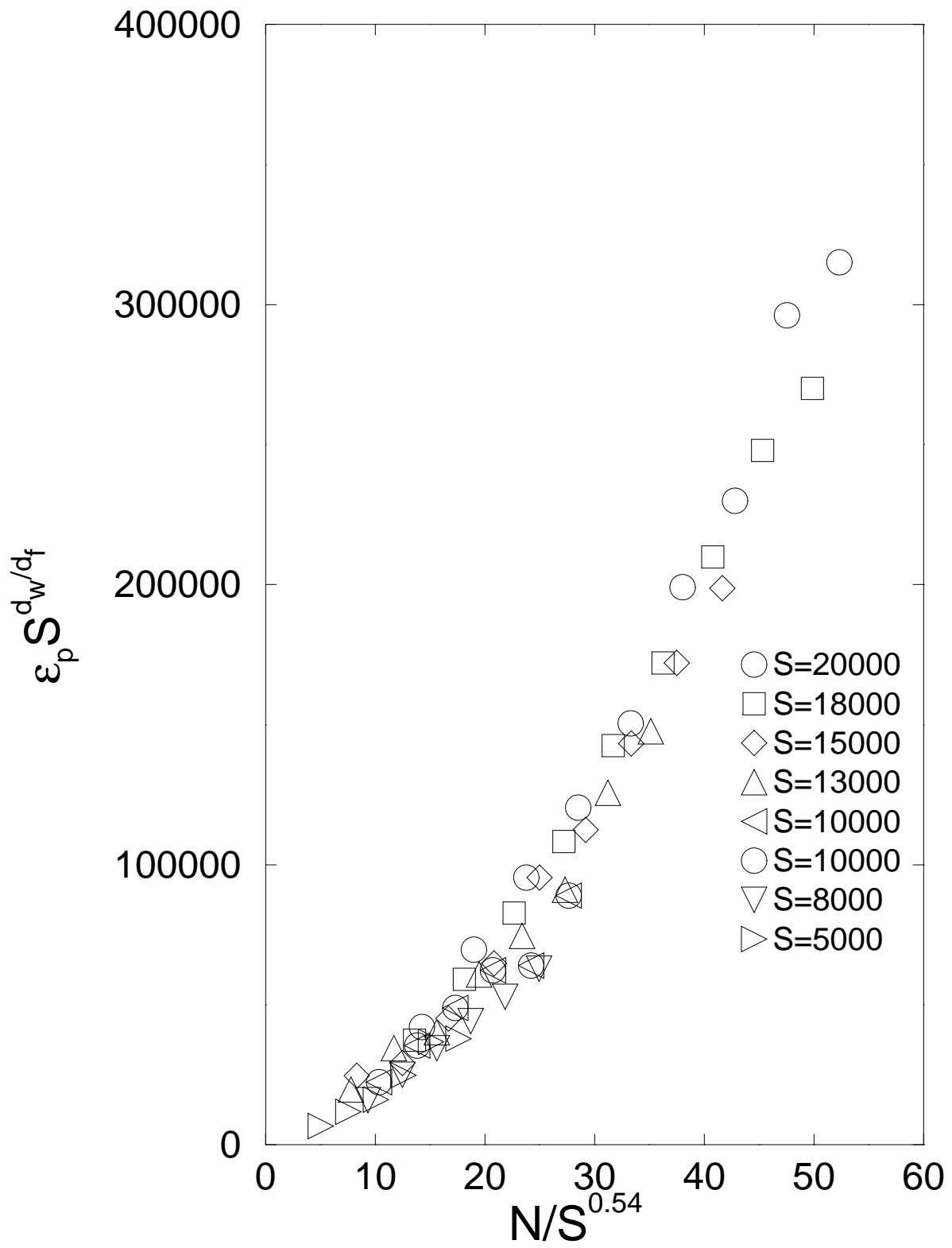


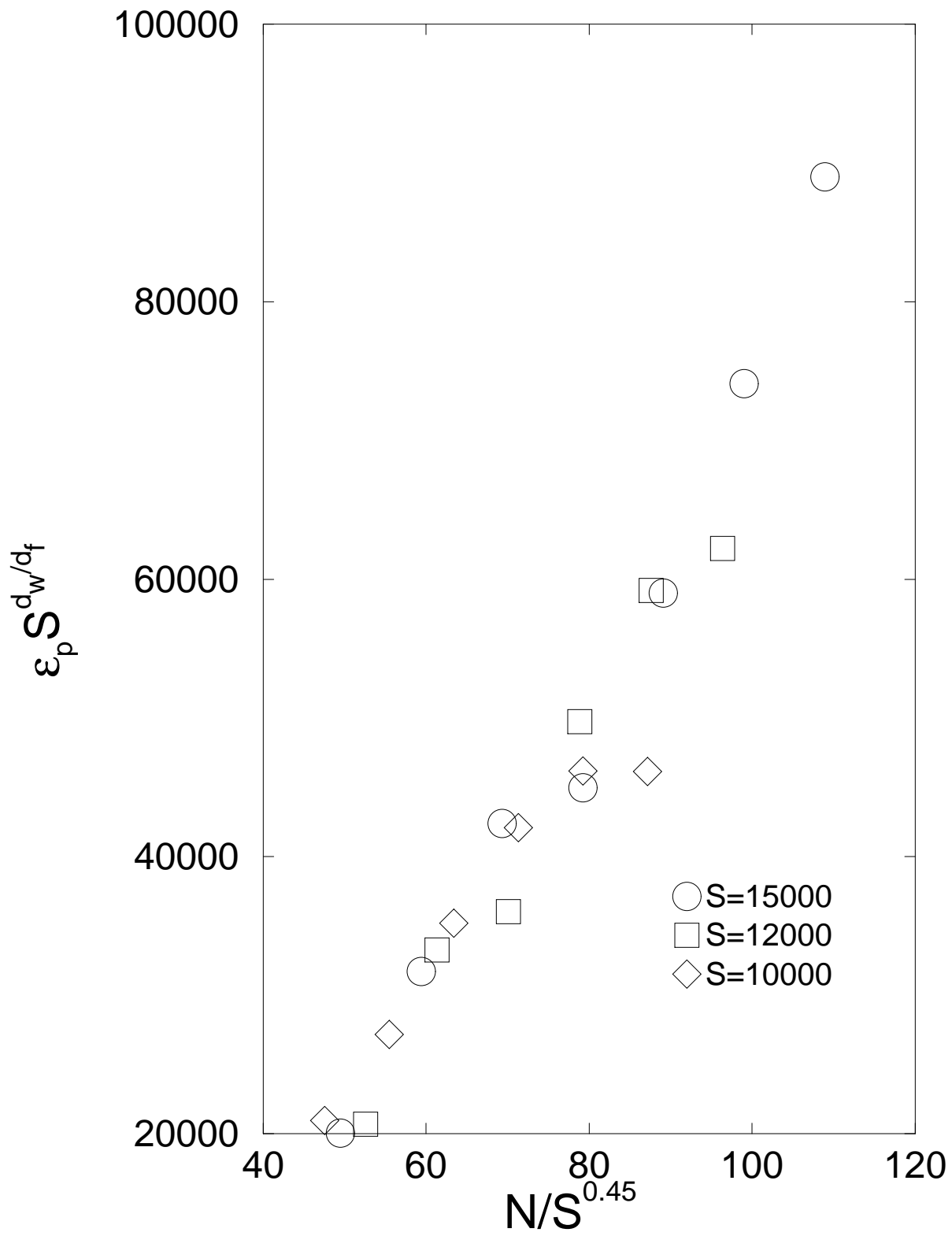














This figure "fig9bw.jpg" is available in "jpg" format from:

<http://arxiv.org/ps/cond-mat/9910138v1>

This figure "fig10bw.jpg" is available in "jpg" format from:

<http://arxiv.org/ps/cond-mat/9910138v1>